JMEPEG (2007) 16:533–538
DOI: 10.1007/s11665-007-9087-2

1059-9495/$19.00

Effect of Powder Type and Compaction Pressure on the Density, Hardness and Oxidation Resistance of Sintered and Steam-treated Steels

Wen-Fung Wang

(Submitted January 18, 2006; in revised form September 21, 2006)

Two types of Hoganas iron powders—sponge (NC), and highly compressible (SC) were investigated. These specimens were compacted with a pressure of 300, 400, 500, 600, and 700 MPa, before sintering in a production belt-type furnace. Steam treatment of the specimens was at 570 °C for 30 min. The sintered density and as-sintered hardness increase with increasing compaction pressure, and are significantly influenced by the powder structural characteristics. During steam treatment the type of powder and compaction pressure have an important influence on the extent of pore closure and weight gain. The maximum hardness was obtained for the components compacted at a pressure of 500 MPa for both groups of iron powders. Surface pore closure and oxidation resistance of the steam-treated components are improved with increasing compaction pressure.

Keywords compaction pressure, hardness, iron powder, oxidation, steam treatment

1. Introduction

The oxidation reaction with steam treatment is commonly used on sintered ferrous parts to achieve the following advantages (Ref 1-4):

(a) improved corrosion resistance;
(b) enhanced hardness and wear resistance resulted from the high hardness of the induced magnetic iron oxide (Fe_3O_4);
(c) complete closure of the interconnected and surface pores;
(d) an economic pore-sealing process as comparing with the copper or plastic impregnation.

One of the advantages of powder metallurgy is that density of sintered parts is easy to adjust by regulating the processing variables such as compacting pressure, sintering temperature, and time. When an impermeable ferrous product is desirable, the sintered parts of high density can be steam-treated to close the surface pores. As the resistance to abrasive wear is important, a layer of oxide up to 5 μm thick can form on all exterior surfaces and also within the interconnected pore network by steam-treating the sintered parts of lower density. The oxide formed within the pore network continues to provide wear resistance after the surface layer has worn away (Ref 5, 6). In addition the oxide layer formed on the sintered iron components is thicker than that on the conventional wrought ferrous parts as being exposed to steam.

Franklin and Davies analyzed the influence of temperature and time of steam treatment on the closure of superficial and interconnected porosity (Ref 7). Razavizadeh and Davies studied the effect of powder type, density, and age hardening on the pore closure and hardness of sintered iron and iron-copper alloys (Ref 8, 9). Volenik et al. investigated the morphology and phase composition of the product of steam oxidation (Ref 10). Molinari and Straffelini reported the effect of steam flow on the nature of the oxide layer as well as their influence on wear and tribological behavior of steam-treated iron (11-13). Mello and Hutchings studied the effect of processing parameters on the surface durability of steam-treated sintered iron (Ref 14). Beiss presented an overview of the thermodynamic and kinetic aspects of steam treatment (Ref 15). Recently, De Mello et al. investigated the effect of compaction pressure and powder particle size on the pore structure and hardness of steam oxidized sintered iron (Ref 16).

The present work investigates two different iron powders of wide uses by local powder metallurgy industry, and studies the influences of powder type and compaction pressure on the density and hardness of sintered Fe-C-Cu alloys, and on hardness, surface morphology, pore closure, and oxidation resistance of the steam-treated components.

2. Experimental

The powders used were supplied by Hoganas Ltd., (a) iron powder NC 100.24 and (b) iron powder of superior compressibility grade SC100.26. The physical properties of the powders are shown in Table 1.

The iron powders were mixed with 0.5 wt.% zinc stearate, 0.4 wt.% natural graphite powder (with a purity of 99% min.)

Wen-Fung Wang, Department of Mechanical Engineering, Southern Taiwan University of Technology, Tainan, Taiwan. Contact e-mail: wfwang@mail.stut.edu.tw.

Table 1 Physical properties of as-received iron powder

Powder	Particle size distribution, %				H_2-loss, %	C content, %	Apparent density, g/cm^3
	−150	−106	−75	−45 μm			
NC	24.9	34.1	24.3	16.7	0.15	0.00	2.35
SC	17.1	31.5	33.3	18.1	0.08	0.01	2.70

and 2 wt.% copper powder (−325 mesh). The powder mixtures were compacted at room temperature with a pressure of 300, 400, 500, 600, and 700 MPa. The resulting compacts, 25 × 25 × 7 mm, were sintered in an industrial moving belt furnace under a cracked ammonia atmosphere ($2NH_3 \rightarrow N_2 + 3H_2$) with a dew point of −30 °C. The total sintering cycle lasted 4 h of which 40 min were spent at the maximum temperature of 1140 °C. The sintering practice is adopted to minimize the distortion of iron-based sintered components that can maintain a dimensional tolerance of 0.05 mm. The sintered specimens were then steam-treated in an industrial batch type furnace. The dimensions of green compacts and sintered specimens were measured with a micrometer. The green and sintered densities were calculated by dividing the weight of specimens by its volume. The specimens were heated, and the superheated steam (120 °C) was conducted into the furnace to purge the air completely. Treatment was carried out at 570 °C for 30 min. Specimens before and after steam oxidation were weighted to an accuracy of 0.1 mg to obtain the weight gain. A Rockwell hardness tester was used for hardness measurement in HRB scale on the outer surface of specimens and each hardness result is the mean of six readings. The hardness tester was made by Sato Seiki Co., Ltd. (Japan) with the model 3R.

Scanning electron microscope (SEM) is a Hitachi (Japan) S-3000N and used to examine the iron powders as-received, the outer surface morphology of specimens in the as-sintered and steam-treated state. Residual interconnected porosity after steam treatment was measured by the oil impregnation method. Oxidation resistance testing of steam-treated specimens was carried out at 250 °C for 100 h. Above 250 °C the oxidation rate of iron has been found frequently to be parabolic. As the films formed by the oxidation of metals thicken, the parabolic relationship becomes the time law most commonly observed (Ref 17). The reported values of residual interconnected porosity and oxidation weight gain are the average of four tested samples.

3. Results and Discussion

3.1 Green and Sintered Densities as a Function of Powder Type and Compaction Pressure

Variation of green and sintered densities with compaction pressure for the NC and SC iron powders is shown in Fig. 1. The green and sintered densities increase with increasing compaction pressure. The SC powder compacts are higher in both green and sintered density than the NC ones, and the density difference between these two types of powders increases with increasing consolidating pressure. Fig. 2 shows the relationship between the green and sintered densities. Sintered density varies linearly with the green density for both types of iron powders. The differing response to compaction of

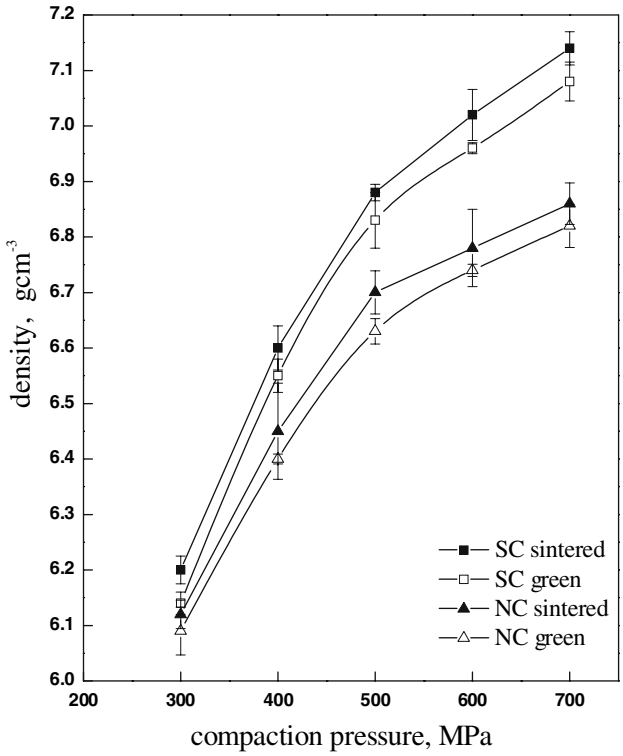

Fig. 1 Variation of green and sintered densities with compaction pressure for the SC and NC iron powders

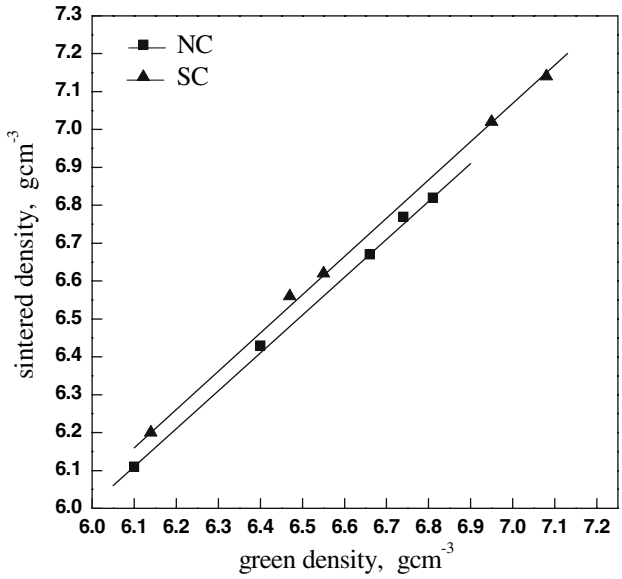

Fig. 2 Relationship between the green and sintered densities of the NC and SC iron powders

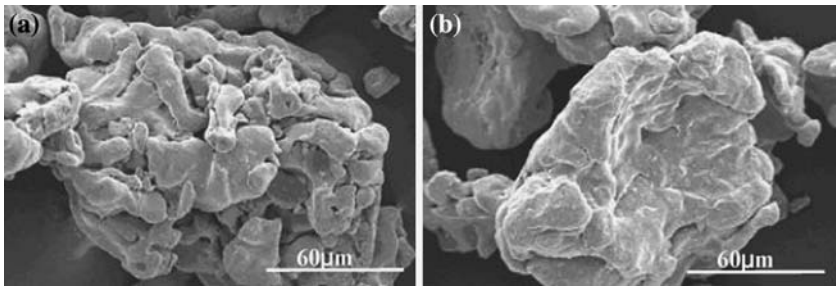

Fig. 3 Surface morphology of NC and SC iron powder (a) NC powder (b) SC powder

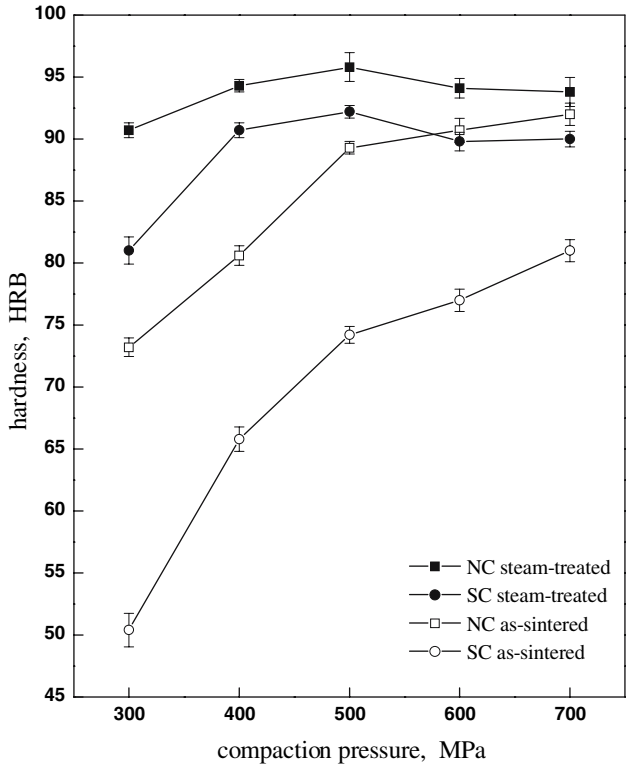

Fig. 4 Variation of hardness with powder type and compaction pressure in the as-sintered and steam-treated state

the two types of iron powder can be explained in terms of the microstructure of powder particles. Figure 3(a) and (b) show the particle morphology of NC and SC powders, respectively. The NC sponge powders look like an agglomerate of fine particles, and are very porous with an apparent density of 2.35 g/cm^3. The SC powder particles are less porous, smoother in outline and approximate closely to a sphere shape. Its apparent density is 2.70 g/cm^3. Due to the less porous characteristics SC powder exhibits higher green and sintered densities than that of NC powders. However, in spite of the different structure and morphology variation of sintered density with green density is similar in trend for both types of iron powders.

3.2 Hardness of As-Sintered and Steam-Treated Components

Figure 4 shows variation of hardness of the as-sintered specimens and the steam-treated batches with the compaction pressure. The principal features are as follows:

1. NC powder compacts are markedly higher in as-sintered hardness than that of SC powder compacts regardless of being lower in sintered density (Fig. 1).
2. After steam-treatment components produced from the SC iron powder obtain a higher hardness increase than those from NC iron powders.
3. The hardness increment of the two groups of specimens after steam treatment decreases with increasing compaction pressure.
4. Steam oxidation is more effective in increasing the hardness of components with lower-sintered density. Due to the less porous characteristics of powder particles the SC specimens exhibit higher green and sintered densities; however, the as-sintered hardness is much lower than that of NC specimens. The explanation can be derived from the compactibility of powders. Figure 5(a) and (d) are the surface morphology of NC and SC compacts after being consolidated with a pressure of 300 MPa and sintered at 1140 °C for 40 min. The compactibility of powder particles can be clearly observed as being consolidated with a lower pressure. Owing to the nonporous and solid features the SC particles are more difficult to be plastically deformed under the compaction pressure, and are loosely packed. Figure 5(d) exhibits many pores, especially large pores, in the SC specimens. The NC powder compacts exhibit a different feature that the particles accommodate each other and are more closely packed. Figure 5(b) and (e) are the higher magnification of NC and SC specimens. Many deep pores typical in the SC specimens shown in Fig. 5(d) can be clearly observed in Fig. 5(e). Figure 5(c) and (f) are the NC and SC sintered alloys compacted with a pressure of 600 MPa. The SC specimen in Fig. 5(f) still reveals its porosity higher than the NC one in Fig. 5(c). Normally, during the hardness measurement the more porous components lead to a larger and deeper indentation, and thus exhibit lower-hardness readings.

After the steam treatment the SC specimens exhibit a higher-hardness increment than the NC ones. For the more loosely compacted specimens there is higher-volume content of interconnected pores for steam penetration; hence a greater amount of Fe_3O_4 oxide can be formed on the surface of these pores, which produces a more effective aid to resist the plastic deformation of indentation during hardness testing. It is the same reason why the hardness increment of the specimens compacted at lower pressure of 300 and 400 MPa is greater than that of those compacted at higher pressure.

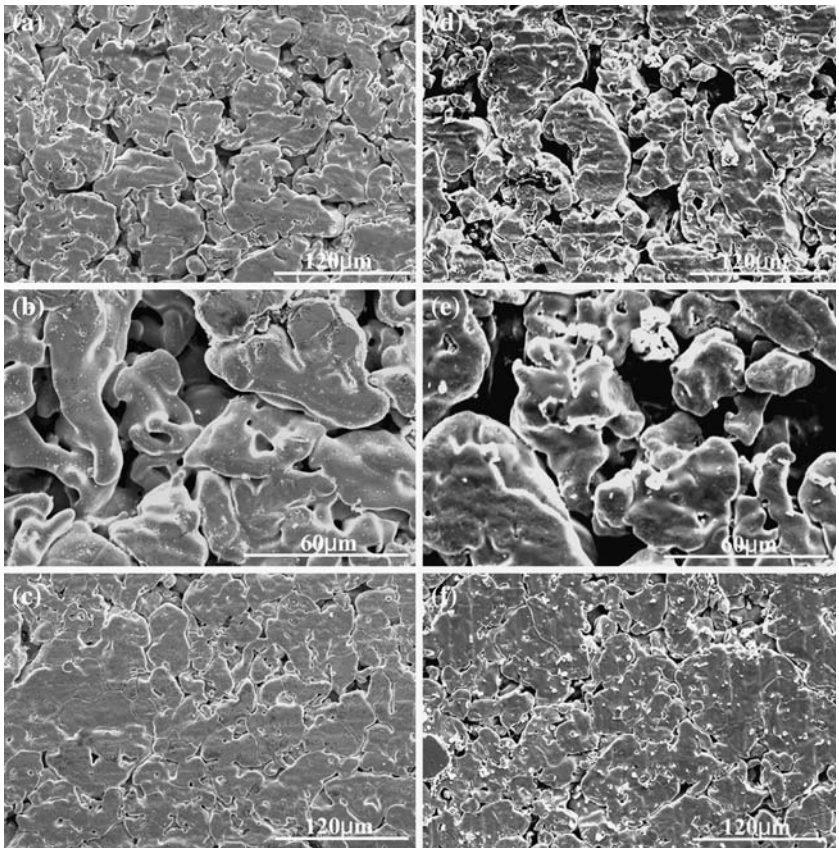

Fig. 5 Surface morphology of sintered NC and SC specimens (a) NC specimen compacted at 300 MPa, (b) pore feature of Fig. 4a, (c) NC specimen compacted at 600 MPa, (d) SC specimen compacted at 300 MPa, (e) pore feature of Fig. 4d, (f) SC specimen compacted at 600 MPa

3.3 Steam Treatment, Pore Closure and Oxidation Testing

Variations of weight gain with the powder type and compaction pressure after steam treatment are shown in Fig. 6. These weight gain data are expressed in weight increase per unit area, where is counted the total bulk surface area of the specimens. The NC specimens obtain a higher-weight gain due to its porous characteristics of powder structure. The weight gain markedly decreases with increasing compaction pressure. As the compaction pressure increases, the particles are plastically deformed heavily. Most pores shrink in volume and small pores are closed. These pores are filled soon by the iron oxide during steam treatment, and the interior steam oxidation is prevented from proceeding further. Therefore, the oxide gain of sintered specimens decreases markedly. Variation of weight gain of sintered specimens with the powder type and sintered density after steam treatment is shown in Fig. 7. Increasing sintered density reduces the weight gain of steam oxidation. For the NC specimens weight gain drastically decreases with the increasing sintered density. Beiss's work shows that the oxide layer is composed of Fe_3O_4, and no copper oxides have been found (Ref 15).

Through comparison of the results in Fig. 4 and 6, it is found that though the magnetite oxide (Fe_3O_4) gain continuously decreases with increasing compaction pressure, the specimens consolidated at a pressure of 500 MPa exhibit the highest steam-treated hardness. To attain high-surface hardness adequate matrix density and volume content of the interior

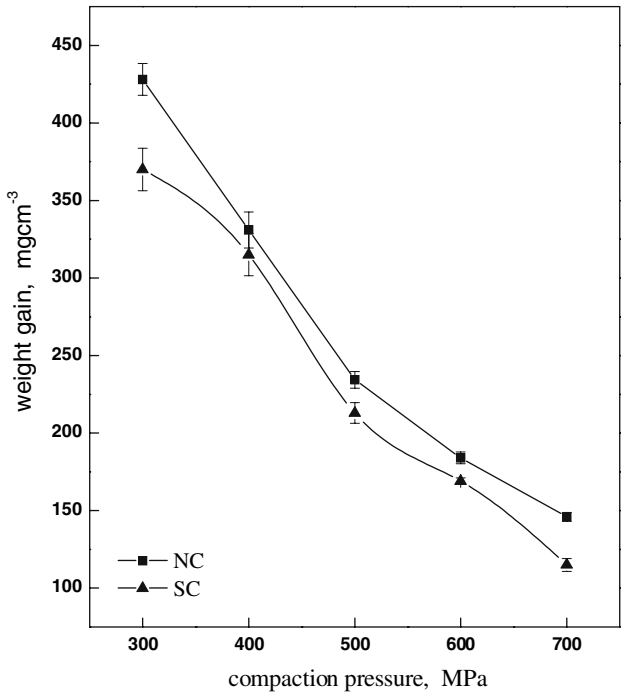

Fig. 6 Variation of weight gain with powder type and compaction pressure after steam treatment

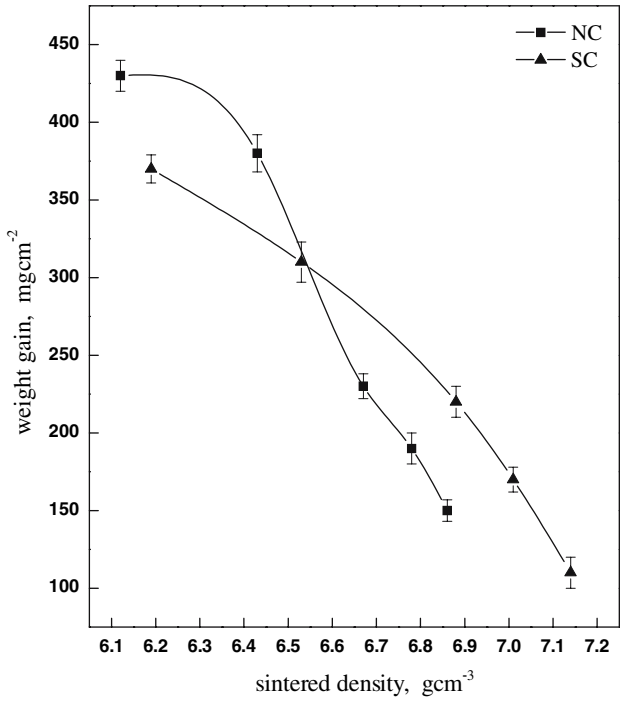

Fig. 7 Variation of weight gain of sintered specimens with powder type and sintered density after steam treatment

Table 2 Residual interconnected porosity of sintered NC and SC specimens

	Steam-treated at 570 °C for 30 min, %				
	300 MPa	400 MPa	500 MPa	600 MPa	700 MPa
NC	2.6	0.9	0.4	0.2	0.2
SC	3.9	1.8	0.7	0.4	0.2

oxide are both required to assist the surface oxide layer to resist the compressive stress resulted from the hardness testing. A higher-initial matrix density results in lower-volume content of interior oxide, therefore, a compromise happens for hardness gain by combination of the matrix density and the volume content of interior oxide. For the components compacted at a pressure of 500 MPa the matrix density and weight gains of interior and surface oxidation seems to be optimum at their best combination, and yield the maximum hardness through the combined effect. As for specimens compacted at a pressure of 600 and 700 MPa interior oxides are virtually not available to increase the bulk hardness.

To examine the effect of powder characteristics and consolidation on the surface pore closure after steam treatment, specimens were vacuum-impregnated with oil. The oil penetrated into the surface interconnected pores. The volume content of open interconnected porosity was obtained by dividing the weight of impregnated oil with its specific gravity. Variation of the residual surface porosity of steam-treated NC and SC specimens with the compaction pressure is shown in Table 2. The residual porosity decreases with increasing compaction pressure. As the pressure is higher than 400 MPa (or the sintered density is greater than 6.4 g/cm^3) the open porosity becomes less than 1%. Most of interconnected pores

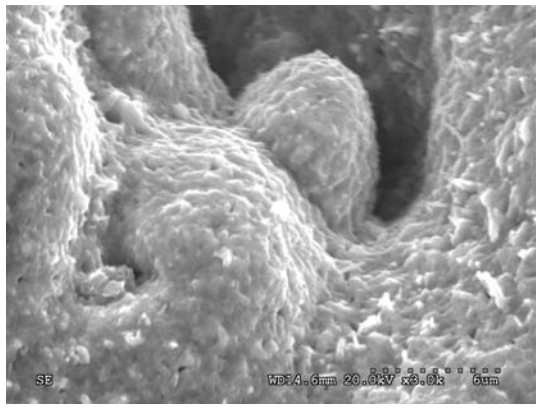

Fig. 8 Surface morphology of the SC specimen steam-treated at 570 °C for 30 min

Table 3 Weight gain of steam-treated NC and SC specimens after oxidizing

	At 250 °C for 100 h, mg/cm^2				
	300 MPa	400 MPa	500 MPa	600 MPa	700 MPa
NC	7.8	4.6	0.7	0.4	0.1
SC	3.5	1.2	...	...	...

were closed. The residual open porosity of SC specimens is higher than that of NC ones, this result agrees well with the suggestion based on the pore structure revealed in Fig. 5(b) and (e).

Figure 8 shows the surface morphology of sintered SC specimens after steam-treated at 570 °C for 60 min. The feature worth to note in this micrograph is that the oxide film contour exhibits a lamella-like feature. And there appear many tiny pores with a diameter less than 1 μm uniformly distributed in the oxide layer.

As shown in Fig. 8 the steam-treated oxide layer is full of very tiny pores. These tiny pores might cause failure of the protective oxide layer during service of the treated components, because the SEM observation of some steam-treated specimens laid in the lab for six months revealed that needle-like oxides stretched out from some of these tiny pores. Therefore, oxidation of steam-treated specimens in air was carried out at 250 °C for 100 h. The weight gains of steam-treated NC and SC specimens after oxidizing are shown in Table 3. The weight gain decreases markedly with increasing compaction pressure. The interior surface area that affords the tiny pores for oxidation decreases drastically with increasing compaction pressure as shown in Table 2. For the SC steam-treated specimens no weight gain can be measured as the compaction pressure is higher than 500 MPa.

4. Conclusions

(1) The powder characteristics have an important influence on the green and sintered densities and hardness of

components. The NC specimens have lower green and sintered densities but higher hardness than SC specimens.

(2) For effective sealing of interconnected pores both NC and SC components should have a sintered density greater than 6.4 g/cm^3.

(3) Both NC and SC samples compacted at a pressure of 500 MPa are the highest in sintered hardness and steam-treated hardness. The maximum hardness is obtained by an optimum combination of matrix density and volume content of interior oxide.

(4) Closure of surface interconnected pore and oxidation resistance of both NC and SC steam-treated components are improved with increasing compaction pressure.

References

1. T.H. Sanderson, Steam Atmosphere Heat Treatment, *Heat Treatment Metals*, 1975, **4**, p 109
2. V.B. Phadke and B.L. Davies, Precipitation Hardening in Sintered Iron-copper Alloys, *Powder Metall. Int.*, 1977, **9**(2), p 64–67
3. "Steam Treated Properties of Sintered Steels, Technical Data Sheet 1031," A.O. Smith Inland Inc., Powder Metallurgy Division
4. A.J. Khan, N.A. Siddiqi, and M. Hamiuddin, Effects of Aging and Steam Oxidation on Sintering Irons and Steels Containing Phosphorus, *Powder Metall.*, 1986, **29**, p 207
5. K. Razavizadeh and B.L. Davies, Effects of Steam Treatment on the Wear Resistance of Sintered Iron and Fe-Cu Alloys, *Wear*, 1981, **69**, p 355–359
6. W.M. de Silva, R. Binder, and J.D.B. de Mello, Abrasive Wear of Steam-treated Sintered Iron, *Wear*, 2005, **258**, p 166–170
7. P. Franklin and B.L. Davies, Effects of Steam Oxidation on Porosity in Sintered Iron, *Powder Metall.*, 1977, **20**, p 11–15
8. K. Razavizadeh and B.L. Davies, Influence of Powder Type and Density on Pore Closure and Surface Hardness Changes Resulting from Steam Treatment of Sintered Iron, *Powder Metall.*, 1979, **22**, p 187–191
9. K. Razavizadeh and B.L. Davies, Combined Effects of Steam Treatment and Age Hardening on Mechanical Properties of Sintered Fe-Cu Alloys, *Powder Metall.*, 1982, **25**, p 11–16
10. K. Volenik, H. Volrabova, J. Neid, M. Seberini, and J. Cirak, Structure of Oxidation Products of Sintered Steel in Superheated Steam, *Powder Metall.*, 1978, **21**, p 149–155
11. A. Molinari and G. Straffelini, Quality Control of Steam Treated Sintered Iron: Importance of Oxide Characterisation, *Surface Eng.*, 1998, **14**, p 331–336
12. A. Molinari and G. Straffelini, Surface Durability of Steam Treated Sintered Iron Alloys, *Wear*, 1995, **181/183**, p 334–338
13. A. Molinari and G. Straffelini, Tribological Steam Treated Ferrous Parts, *Int. J. Powder Metall.*, 1997, **33**(5), p 55–62
14. J.D.B. De Mello and I.M. Hutchings, Effect of Processing Parameters on the Surface Durability of Steam-oxidized Sintered Iron, *Wear*, 2001, **250**, p 435–440
15. P. Beiss, Steam Treatment of Sintered Parts, *Powder Metall.*, 1991, **34**, p 173–178
16. J.D.B. De Mello, R. Binder, A.N. Klein, and I.M. Hutchings, Effect of Compaction Pressure and Powder Grade on Microstructure and Hardness of Steam Oxidized Sintered Iron, *Powder Metall.*, 2001, **44**, p 53–58
17. O. Kubaschewski and B.E. Hopkins, *Oxidation of Metals and Alloys*. Butterworths, London, 1967